RSC Advances

ROYAL SOCIETY OF CHEMISTRY

www.rsc.org/advances

Journal Name

ARTICLE

Acid catalysed cross-linking of poly vinyl alcohol (PVA) by glutaraldehyde: Effect of crosslink density on the characteristics of PVA membrane used in single chambered microbial fuel cell

Received 00th January 20xx,
Accepted 00th January 20xx

DOI: 10.1039/x0xx00000x

www.rsc.org/

Ruchira rudra[a], Vikash Kumar[a], Patit Paban Kundu[*]

Abstract

In the present study, acid catalysed cross-linking of poly vinyl alcohol (PVA) with varying concentrations of glutaraldehyde was analyzed and the cross-linked PVAs were utilized as membrane separators in single chambered microbial fuel cells (MFCs). PVA with varying concentrations (1, 2, 4 and 6%) of glutaraldehyde have resulted in a respective 2.8, 5.6, 32 and 34% of degree of cross-linking in PVA1, PVA2, PVA3 and PVA4 membranes. Due to the reduction of available free volume in membranes, progressive improvements in membrane rigidity with impeded membrane porosity were observed with increasing cross-link densities. In succession, proton conductivities of 7.53×10^{-3}, 8.4×10^{-4}, 1.2×10^{-4} and 4.5×10^{-5} Scm^{-1} were observed from the respective PVA1, PVA2, PVA3, and PVA4 membranes. The increased cross-link density enhanced the mechanical strength but reduced other membrane properties such as water uptake and proton conductivities of the membranes. Further, the casted membranes were assembled as MEAs in open air cathode MFCs where, a maximum power and current density of $119.13 \pm 6 mWm^{-2}$ and $447.81 \pm 18 mAm^{-2}$ were observed from PVA3 fitted MFC, using mixed firmicutes as biocatalysts. With increased cross-link density, higher ohmic resistances were observed in MFCs, but due to lower oxygen diffusion in anode, increased performance were observed from highly cross-linked membranes. Electrogenic firmicutes revealed an overall ~93.45% of COD removal in 27 days operation, indicating the efficiency of respective membranes as separator in MFCs. In general, the study depicts the relevance of different acid catalysed cross-linked PVA membranes in bio-energy conversion from microbial fuel cell.

INTRODUCTION

Fuel cells, being a promising clean energy source, efficiently generate electrical energy at low environmental cost from widely available chemical energy sources. Microbial Fuel Cell (MFC), being one such electrochemical device, converts chemical energy contained in organic matter e.g. glucose, fructose etc. into electricity through the catalytic (metabolic) activity of microorganisms [1-2]. In order to enhance the columbic efficiency, different separators are used to avoid the direct electrodes contact, avoiding short circuit in the system. Generally, any ion permeable material can be employed as a

barrier which can serve as PEM in fuel cells; the best known example is Nafion 117. As an alternative, S. Ayyaru developed a sulfonated polystyrene-ethylene-butylene-polystyrene (SPSEBS) membrane, which was found to be producing approximately 106.9% higher power density in comparison to Nafion 117 in a single chambered MFC [3]. In another instance, sulfonated polyether ether ketone (PEEK) showed an approximate 55.2% higher power density over Nafion-117 membrane [4]. Using *Shewanella putrefaciens*, a maximum voltage of 0.676 V and 0.729 V with a power density of 39.2 - 7.39 mW/m^2 and 57.8 - 5.5 mW/m^2 was observed respectively with Nafion and Ralex membrane [5]. Similarly, different low cost materials such as earthen pot have widely been studied to reduce the overall fabrication cost [6]. In comparison, Kim et al equated cation-exchange, anion exchange, and ultra filtration (molecular cut-offs of 0.5, 1, and 3 kilodaltons) membranes to determine their effect in MFC performance [7-9]. Many studies on surface modification of polyolefins, (e.g. by sulfonation, photosulfonation, plasma treatment, radiation grafting etc.) have been conducted for the enhancement of hydrophilicity, adhesion, and other membrane properties. Different studies have been performed on the surface sulfonation of polyethylene film using oleum and chlorosulfonic acid [10-14]. Likewise, the inherent hydrophilicity of poly vinyl alcohol (PVA) makes it an attractive polymer for water treatment application, where adequate cross-linking ensures compaction under pressure [15]. In some of the previous works, different cross-linking agents have been used to serve this purpose. Hou *et al* have used sulfosuccinic acid as a primary cross-linker in PVA film [16]. Moon-Sung Kang and his group have utilised poly (styrene sulfonic acid-*co*-maleic acid) as well as glutaraldehyde (GA) in order to build up the chemical network structure in PVA film [17]. In order to enhance the proton conductivity of the PVA film, sulfophthalic acid (sPTA), sulfoacetic acid is used as sulfonating as well as cross-linking agent [18, 19]. The effect of cross-linking by Maleic acid on PVA film was also reported [20].

In the present work, we have explored the suitability of PVA film cross-linked by glutaraldehyde (GA) under acidic condition as a membrane in single chambered microbial fuel cell in the form of a membrane electrode assembly. Pure PVA is excessively hydrophilic in nature and also insulating material (with lower ionic conductivity) [21]. Due to the proper cross-linking of the hydroxyl groups present in PVA, the water uptake value and swelling ratio can effectively be controlled. In the present study, GA is used in different proportions to crosslink PVA under acidic condition. The cross-linked PVA membranes are characterized by ATR-FTIR, X-ray diffraction (XRD) and thermo gravimetric analysis (TGA); cross-link density of the membranes are measured to determine their suitability for bio-energy production in MFCs.

RESULT AND DISCUSSION

Fourier Transform Infrared (FTIR) analysis

FT-IR spectra of pure and cross-linked PVA membranes showed differences in characteristic functional groups with

the increase in crosslink density (Figure 1). The characteristic peaks appearing at 3350 cm^{-1} was assigned to –OH stretching due to the strong inter and intra molecular hydrogen bonding in PVA membranes. In addition, carbonyl peak stretching at 1723 cm^{-1} and acetal linkage (-C-O-C-) stretching vibrations near 1087 cm^{-1} were observed in cross-linked PVA membranes. The characteristic absorption bands at 2925 cm^{-1} corresponded to the asymmetric and symmetric stretching vibration of $–CH_2$ groups [22, 23]. With increasing contents of glutaraldehyde in membranes, reduction in absorbance peak intensities at 3350 cm^{-1} was observed. This was indicative of the reduced concentrations of the hydroxyl groups, left after the cross-linking reaction. The peak due to the C-O-C stretching shifted towards higher frequency regions due to the formation of bound C-O-C of acetal and ether linkages, as a result of the reaction between the hydroxyl groups and the cross-linker, glutaraldehyde. With increasing GA content in the membranes, more hydroxyl groups were consumed and more acetal rings and ether linkages were formed as a result of the crosslink formation. In addition, to accelerate the rate of cross-linking reaction, H_2SO_4 as a catalyst, methanol as a quencher, and acetic acid as a pH controller were used. Since, pristine PVA is highly hydrophilic and unstable in aqueous medium, it was cross-linked in order to optimize the strength and performance of the membrane (as PVA1, PVA2, PVA3 and PVA4 membranes). The corresponding feeble peak intensities with increasing contents of cross-linker, glutaraldehyde, confirmed the cross-linking of PVA membranes with subsequent hindrance towards water.

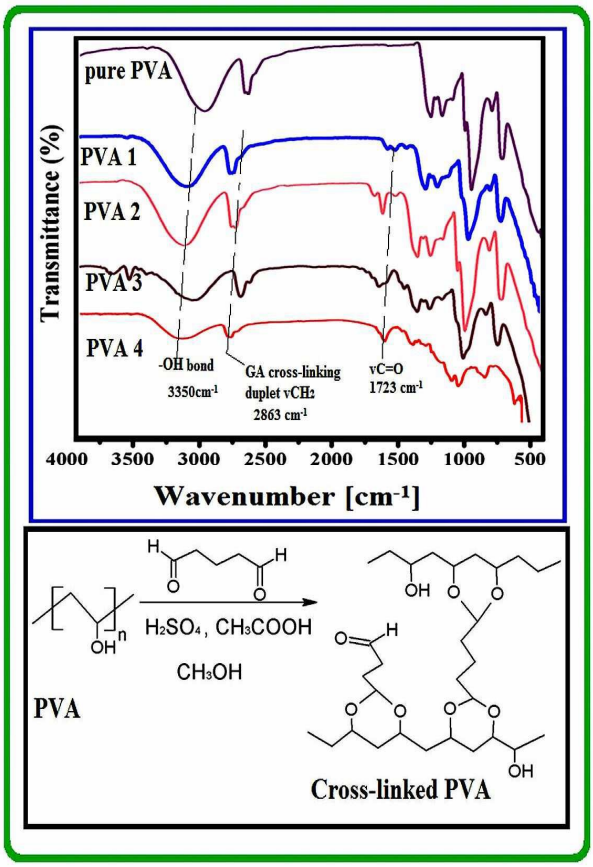

Fig 1: FT-IR spectra of membranes

Analysis of Crosslink Density, Water Uptake and Swelling ratio

For cross-link density analysis, the gel fractions of different membranes were calculated using eq. (1), where a rise in crosslink density was observed due to the increase in the content of crosslinker (GA) with a maximum cross-link degree of 34% for PVA 4 membrane. With other cross-linked networks, a respective cross-linking density of 2.8 %, 5.6% and 32% were observed from PVA1, PVA2 and PVA3 membranes. Increasing GA has resulted in maximum crosslink density in PVA4 membrane as the cross-linker generates an acetal ring linkage over most of the outer surface

of the membrane, forming a hydrophobic protective layer [16]. The corresponding water uptake values for all the samples were calculated using eq. (2). PVA, being highly hydrophilic does not account much in terms of membrane stability and strength. Reductions in hydrophilicity with increased mechanical strength were observed in membranes with increased degree of crosslinking. Respective water uptake values of 515, 292, 142 and 132% were observed for the casted PVA1, PVA2, PVA3 and PVA4 membranes, where with an increase in the GA content, the water uptake of the PVA membranes was found to decrease; the least water uptake was observed for PVA4 membrane (Figure 2). The reduced hydrophilic nature of PVA with increased cross-links entailed orientation of symmetrical channels within membranes, resulting in higher mechanical strengths with reduced water retention in membranes. Also, greater constraints imposed by higher cross-linking eventually allowed fewer water molecules to get entrapped in the pores of the membrane. As a consequence, this reduced available free space in the membranes proportionally lowered the water uptakes in highly cross-linked membranes (PVA 2, 3, and 4 membranes) over PVA1 membrane.

In order to rationalize these results, swelling behaviour was studied. The corresponding swelling values were calculated from eq. (3). The swelling ratios for PVA1, PVA2, PVA3 and PVA4 membranes were 275, 183, 70 and 56% respectively. The observed decrease in the swelling ratio of PVA3 membrane compared to that obtained for PVA1 and PVA2 membrane was due to the above mentioned reason. With the increasing content of GA, the membrane rigidity increased that resulted in comparatively lower swelling ratios in membranes. In effect, GA incorporation resulted in restricted inter chain mobility and reduced available free volume space that allowed lower water uptake and swelling ratios in the casted membranes. Nevertheless, these provided a promising aspect for PVA membranes in PEM application with reduced water uptake and swelling ratios.

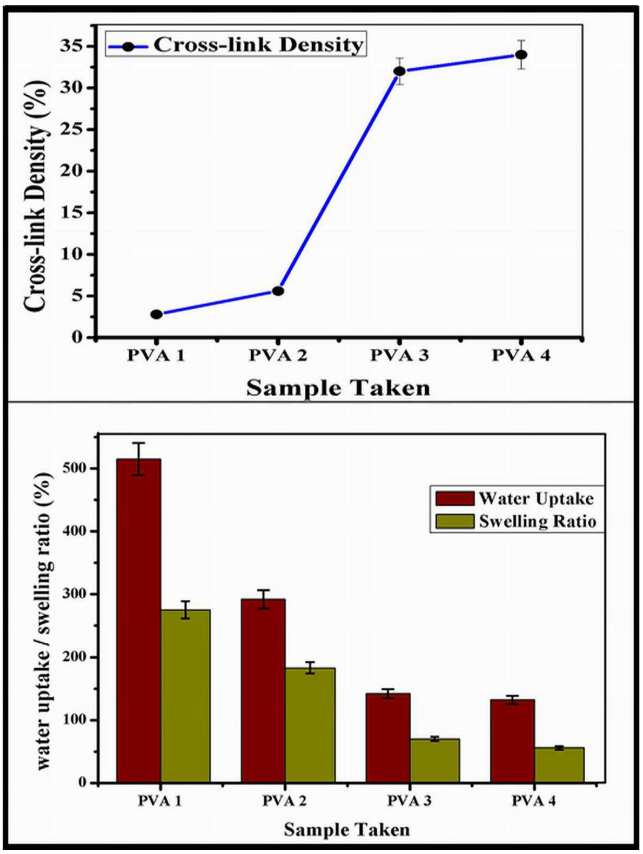

Fig 2: Crosslink density, water uptake and swelling ratios of PVA membranes

Analysis of ion exchange capacity and proton conductivity

Ion-exchange capacity (IEC) of a membrane defines its ability to displace ions initially attached/incorporated in its structure by an oppositely charged ion present in the surrounding solution. After titration, the IEC values of the respective membranes were obtained (Figure 3). The IEC for the casted PVA1, PVA2, PVA3 and PVA4 membranes obtained from the protocol 1 i.e. treating with 1 M H_2SO_4 followed by titration with NaOH were 0.25 meq g^{1}, 0.23 meq g^{-1}, 0.19 meq g^{-1} and 0.16 meq g^{-1} respectively; these results were observed to be low in comparison to that reported in the literature for PVA membrane [24]. The structure of PVA indicates that it has no polar group which can ionize to form protons. From the structure of PVA with only hydroxyl groups, one can predict that it should not show any ion exchange capacity. The observed low values of ion exchange capacities of these membranes originate from the entrapped hydronum ions, penetrated during long (24 hours) of sulphuric acid treatement; repeated washing can only remove the hydronium ions attached at the surface or just beneath the surface of the membrane. The observed IEC values clearly indicate about the inverse correlation between IEC and GA cross-linked PVA structure. The least cross-linked structure (PVA1) showed higher IEC, whereas with increasing glutaraldehyde concentration, reduction in IEC with increased cross-linking was observed. These results indicate that the less crosslinked structure allows more penetration of hydronuim ions to the bulk of the membrane, thereby retaining more hydronium ions during washing. As per protocol 2 of measuring IEC, the membranes were treated with 1 M NaCl solution, followed by titration with NaOH solution. In this process, there is no scope of entrapment of hydronium ion inside the crosslinked PVA membranes (as observed in protocol 1). The IEC values obtained in this process are almost zero (Fig. 3). These results are in conformity with the structure of PVA in which only hydroxyl groups are present (absence of any polarizable group like sulfonic acid) [25].

For proton conductivity measurement, the protons need to pass through the membrane from its one side to another one. Enhanced proton conductivities with a respective value of 7.53×10^{-3}, 8.4×10^{-4}, 1.2×10^{-4} and 4.5×10^{-5} were observed from PVA1, PVA2, PVA3 and PVA4 membranes. In case of PVA3 and PVA 4 membranes, reduction in proton conductivity was observed with respect to PVA1 and PVA2 membranes. The reason was the higher GA concentration, which limited the available free volume in membranes required for ionic mobility in the membrane with increasing cross-linkages. Proton hopping depends directly on the available free space, where GA concentration regulated the membrane porosity, influencing the overall IEC and proton conductivity in the membranes. As observed earlier, increasing GA concentration increased the rigidnessof the membranes which eventually allowed lower water uptake with restricted transverse ionic conduction. These varying effects of cross-linked PVA membranes were further dealt in MFCs for testing their efficiency.

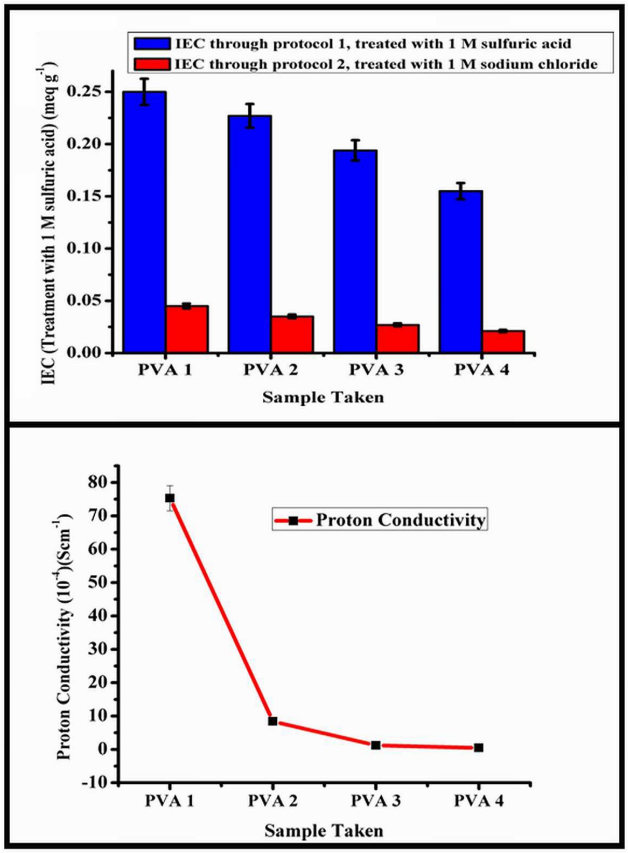

Fig 3: Ion exchange capacities and proton conductivity of the casted PVA membranes

Analysis of morphology and mechanical integrity

SEM analysis of acid catalyzed cross-linked PVA films revealed decreased porosity in all membranes with increasing GA incorporation (Figure 4). Increased rigidity in highly cross-linked membranes (PVA3 and PVA4) resulted in higher compact membrane with feeble porosity. This increased cross-linking reduced the available free volume in the membrane and allowed stiffness at a low pH with the formation of acetal covalent linkages in the membranes. With the use of X-ray diffraction method, different cross-linked PVA membranes were analyzed on normal plane (Figure 5).

The diffraction peak of PVA membrane at 2θ of 19.9° was observed due to the (101) and $(10\bar{1})$ crystal planes [26]. The semi crystalline nature of the casted PVA membranes was enhanced by the intermolecular H-bonding where a characteristic decrease in peak height was observed. This was attributed to the reduction in crystallinity with an increase in the cross-link density of the membrane. Increasing crosslink density increased amorphousness in PVA 3 and PVA 4 membranes which showed reduced peak heights. On the other hand, PVA2 and PVA3 membranes showed relatively sharper peaks at (101) planes. In effect, membrane amorphousness was directly influenced with the crosslink density, where altered semi crystalline nature was observed with the presence of increasing cross-linkages. In a related study, thermal degradation behaviour of the membranes was studied with thermo gravimetric analysis (TGA) (Figure 6). Increasing crosslink density resulted in increased degradation temperature and decreased weight loss of the membranes. In a three step degradation process, the first step allows the breakage of cross-links, where approximately 60% weight loss in PVA1, 55% in PVA2, 50% in PVA3 and 40% in PVA4 was observed. In the second and third step, further degradation of inter-component bonds by breaking of the side chains and finally the actual cleavage of the polymeric backbone was conducted [27, 28]. The results obtained here indicated that the mobility of the polymer segments at the interfaces of PVA and GA was suppressed by strong cross-linked interactions, which showed improved thermal stability with higher cross-linked membranes. In effect, the tensile strength and percent elongation of the cross-linked

membranes at their failure point were observed (Figure 7). The tensile strength of 20 MPa with a percent elongation of 480% was observed with pristine PVA membrane [21]. Here, with the increasing crosslink density, the mechanical strength of the membranes was found to increase, showing a maximum tensile strength of 30 MPa in PVA3 membrane. This resulted in increased tensile strength where the percent elongation at break decreased with the increasing crosslink density. The % elongation values of PVA 3 and PVA4 was found to be 45.2 and 40 respectively. This enhancement in tensile strength and decrease in percent elongation was attributed to the formed cross-linked networks, which restricted the mobility of the polymer chains in membranes.

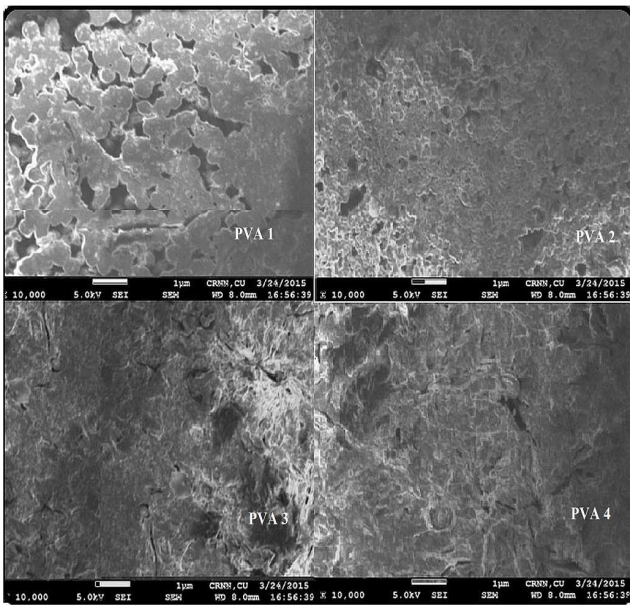

Fig 4: FE-SEM image of cross-inked PVA membranes

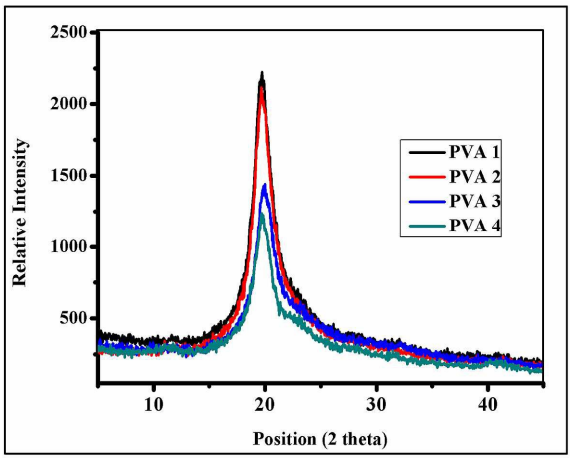

Fig 5: XRD patterns of cross-linked PVA membranes

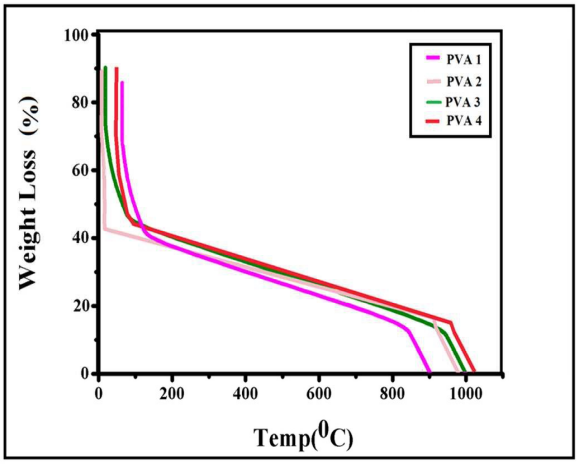

Fig.6. TGA curves for the cross-linked PVA Film

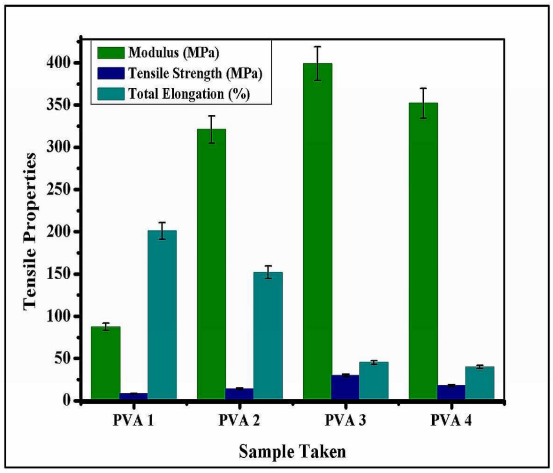

Fig.7. Tensile, elongation and modulus of cross-linked PVA membranes

Oxygen diffusivity across membrane

Oxygen diffusivity across the membranes was analyzed in order to study the periodic variations in the content of dissolved oxygen. Increased oxygen flux from cathode to anode ensued a respective mass transfer coefficient of 2.1 × 10^{-2} cm s^{-1}, 6.45 × 10^{-3} cm s^{-1}, 1.5 × 10^{-3} cm s^{-1} and 1.74 × 10^{-4} cm s^{-1} from PVA1, PVA2, PVA3 and PVA4 membranes (Figure 8). A direct correlation existed between oxygen permeability and the degree of cross-links in the membrane, where maximum oxygen pervasion was observed in least cross-linked PVA1 membrane. The reason was attributed to the increased inter volume spatial structure of the membrane that allowed more oxygen to diffuse in the chamber. In contrary, PVA3 and PVA4 membranes with the presence of increased cross-linkages showed reduced oxygen permeability in comparison to PVA1 and PVA2 membranes. In comparison, approximately 88%, 96%, and 98% lower mass transfer (oxygen influx) from PVA4 were observed over respective PVA3, PVA2 and PVA1 membranes. In effect, with other membrane parameters like IEC and proton conductivity involved, influence of increased oxygen permeation were further assayed in MFC application.

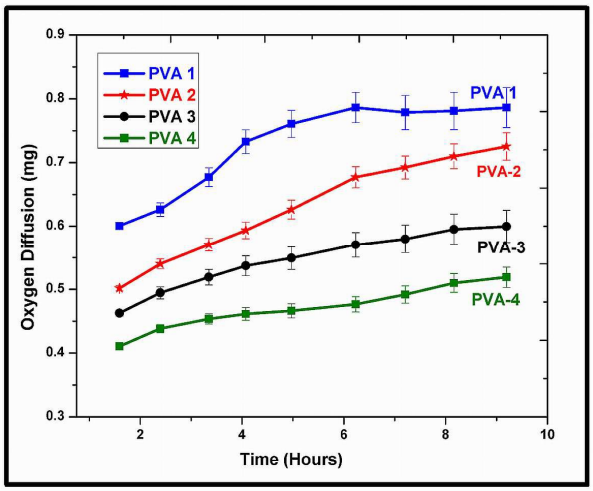

Fig.8. Oxygen Diffusion reaction of the membranes

MFC Performance

All four MFCs were monitored under similar operating conditions. The cathodes were initially kept covered with parafilm to establish a favourable anodic start-up environment where, external resistances were avoided to augment the microbial catalytic activity for rapid potential development without draining energy out of the system. With random fluctuations, an average anode and cathode potentials of -222 mV and +174 mV were observed with Ag/AgCl as reference electrode (data not shown here). After acclimatization, the system showed gradual OCV (open circuit voltage) increments, indicating a maximum open circuit potentials of 611±20 mV, 549±30 mV, 501±18mV and 401±12mV from MFC-A, B, C and D respectively (Figure 9); MFC A, B , C and D were fitted with PVA1, PVA2, PVA3 and PVA4 respectively. The obtained OCVs were directly influenced by the respective crosslink density of the membranes, where increased water uptake with lower crosslink density resulted in excessive air intrusion in anode chamber, generating cross potentials between anode and cathode. As a result, despite of

increased IEC and proton conductivity, cross potentials in MFC-A and B were reverse biased and showed feeble OCVs with PVA 1 and 2 membranes. In comparison, increased crosslink density with constricted membrane pores in PVA3 and 4 resulted in enhanced OCVs due to the lower air reflux in anode from cathode in case of MFC-C and D fitted with PVA 1 and PVA 2 membranes. Here, MEA had an added effect, where close electrode spacing increased the cell efficiencies because of the reduced in -between electrolyte resistances [29]. Increased drop in voltage and current was observed in MFC-C over other units, where fitted PVA3 membrane efficiency was evident over other employed membranes (S1 supporting information). A maximum respective current of 0.141 mA, 0.174mA, 0.216mA and 0.243mA was observed from MFCs (A-D) at 1150 Ω. Increased cross-link density in PVA4 with least proton and ionic conductivity, showed better OCV and current over PVA1 and PVA 2 membranes. But, altogether the performance was lower than PVA3 membrane. This is attributed to its relatively constricted membrane pores that allowed lower ionic conduction over PVA3 membrane. The lower efficiency in terms of OCV and current generation in PVA1 and PVA 2 is due to the higher oxygen influx from cathode to anode in MFC-A and MFC-B. With varying resistors in descending range, polarization curves were obtained for all MFCs (Figure 10). Increased activation losses (i.e., energy lost in initiating the redox reaction, indicating the charge transfer from cell to anode) with frequent voltage drops were observed at higher resistances. At lower resistances, increased voltage drops, indicative of increased electron flow within the circuit were observed. In overall, a maximum power and current density of 119.13 ± 6mWm^{-2} and 447.81 ± 18mAm^{-2} were observed from MFC-C (with PVA3 membrane). Comparatively, a respective power and current density of 41.88 ± 3mWm^{-2} and 246.37 ± 15mAm^{-2}, 62.15 ± 2mWm^{-2} and 297.43 ± 11mAm^{-2}, and 97.65 ± 0.5mWm^{-2} and 376.81 ± 3mAm^{-2} were observed for MFC-A, B and D.

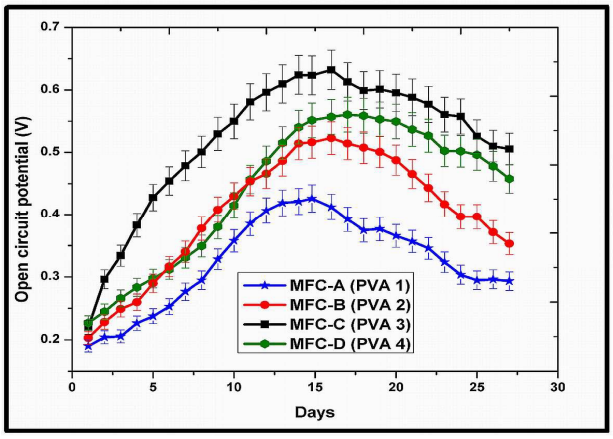

Fig.9. Open circuit potential of MFCs

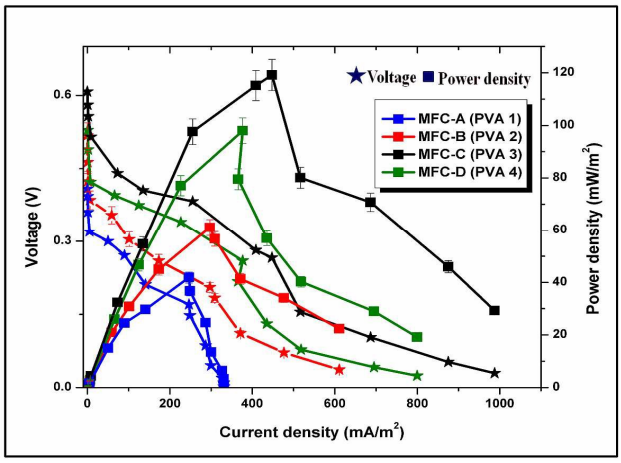

Fig.10. Polarization curves of MFCs

In effect, an approximate 63%, 48%, and 18% of increased power output was observed from MFC-C over other respective MFCs. Optimum cross-linkage was found in PVA3 membrane that ensured lower mass transfer of oxygen from

cathode to anode. This, in turn, aided in enhanced MFC-C performance over other membranes fitted MFCs. In MFC-D, lower power output was observed. This result was expected because of relatively reduced IEC and proton conductivity of PVA4 with highly constricted pores in the membrane structure. In general, the obtained power output was compared with other relevant studies, to indicate the effectiveness of cross-linked PVA membranes in MFC application (Table 1 Supporting Information). Different lower cost materials as PEM have shown reduced efficiency than cross-linked PVA membranes, featuring its potential MFC application as a low cost membrane.

Electrochemical Impedance Spectroscopy (EIS) Analysis

For internal resistance (R_{in}) measurement of the whole unit, anode was connected to the working electrode whereas both reference and counter electrodes were connected to the cathode terminal. Nyquist graphs were plotted from EIS analysis, where specific resistance components for MFCs were calculated (Figure 11). The internal resistance (R_{in}) of the whole system was segmented in various specific components like activation resistance, ohmic resistance (R_m- attributed to electrode resistance, membrane resistance, etc.) and concentration resistance [30]. The ohmic resistance, R_m, as calculated using the equivalent circuit (S2 supporting information), were found as ~ 3.6Ω for MFC-A, ~8.7Ω for MFC-B, ~ 12.3Ω for MFC-C, and ~17.4Ω for MFC-D. Minimal ionic resistance was observed in MFC-A (with fitted PVA1 membrane), where low cross-link density and less compact structure with less constricted pores in PVA1 membrane allowed abundant transverse ionic conduction across MEA. A substantial increase in ohmic resistance from MFC-B to MFC-D was observed, revealing higher membrane impedance due to increased charge transfer hindrance across the membranes. Nevertheless, it was expected that on moving from PVA 1 to PVA 4, the cross-link density would increase, leading to an increase in the charge transfer resistances with minimal ionic conduction. However, despite of this increased internal resistance, the minimal ionic conduction due to the restricted pores in highly cross-linked membranes of MFC-C and D relatively reduced the generated cross potential, resulting in enhanced electrical performance of PVA3 and PVA4 over PVA1 and PVA2 membranes.

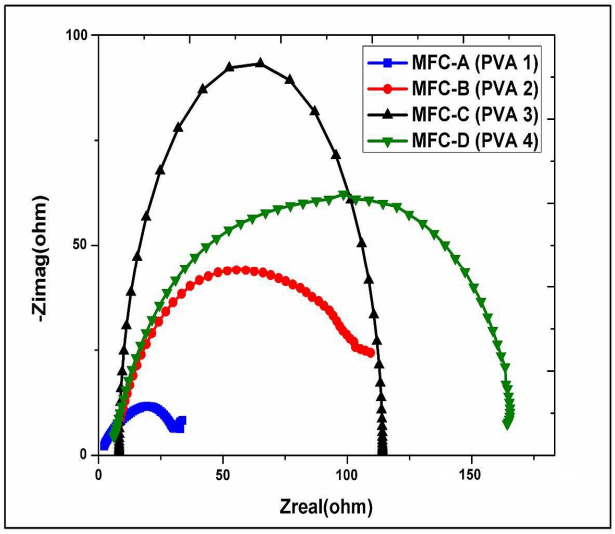

Fig.11. Electrochemical impedance spectroscopy (EIS) diagram

Biofilm growth on electrode surface

Microbial growth is generally associated with bio-film adhesion due to the EPS (exo-polysaccharide) present on the microbial cell-wall. SEM analysis revealed predominant microbial colonies associated at the surface of electrode

(carbon cloth); these colonies were evidently engaged in the electrochemical reaction at the anode (Figure 12). In order to enumerate the microbial electrochemical potency, cyclic voltammograms with and without bio-film, were performed in a 15mL Bob cell (Gamry Instruments., USA) at a scan rate of 2mV/s (Figure 13).

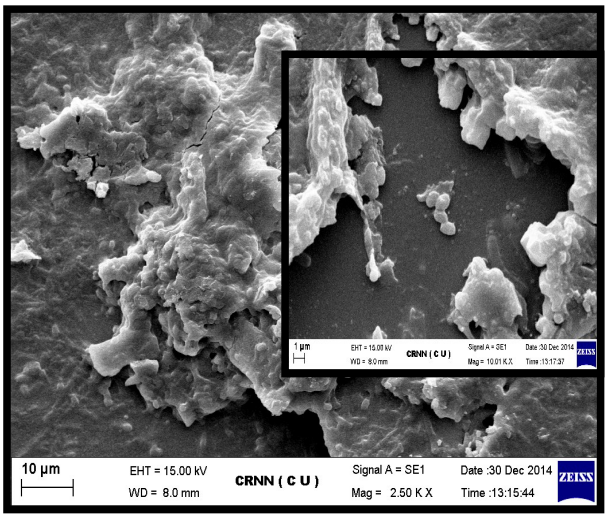

Fig.12. SEM images of bioelectricity-producing mixed consortia on electrode surface.

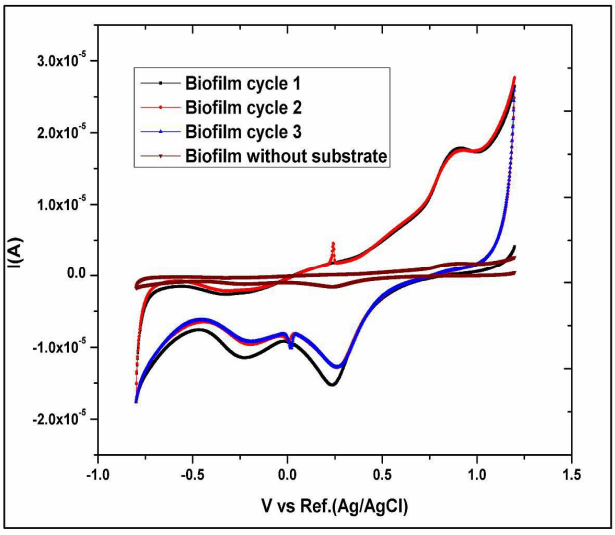

Fig.13. Cyclic voltammograms of biofilm and control

Electrochemical activities were found to be absent in bacterial devoid medium, as no observable redox peaks were observed in the control experiments (using PBS buffer solution). On the other hand, the presence of bio-films revealed prominent redox activities with an oxidation peak at 889 mV vs. ref. at 10.3 µA, and two distinct reduction peaks at 222 mV and -262 mV vs. ref at -10.6 µA and -7.9 µA respectively. The oxidation was indicative of electron transfer from electrode to biofilm, whereas reduction peaks corresponded to the charge transfer from bio-film to electrode. The plausible reason for this electrogenic activity could be attributed to the microbial cell surface proteins that ensured its bio-catalytic potency for sustained substrate oxidation on repeated potential cycling.

COD Removal

In order to ensure the substrate oxidation rate, routine analysis of anolytes were conducted. In effect, a respective COD removal of ~93.45%, ~90.18%, ~85.15%, and ~81.24% were observed from MFC-A to D from 150 mg/L anolyte in 27 days run (Figure 14). These variations were primarily due to the individual membranes employed in these units. MFC-A showed highest energy recovery as the employed PVA1 membrane showed increased oxygen diffusion from cathode, allowing direct substrate oxidation with respect to other employed membranes. In comparison, minimal ionic conduction from MFC-C and and MFC-D, despite of increased electrical performance from these units showed lower COD removal, because the employed membranes were found to show a relatively higher cell impedance. The lower current extract, oxygen diffusion from cathode, polarity, IEC

and proton conductivity aided in lower COD removal, but these parameters also aided in the increased performance in MFC-C and MFC-D. Generally, COD removal is largely influenced by the employed microbes and it is necessary to keep them electrogenetically active for sustained substrate utilization. In many cases, microbial sustenance gets adversely affected with oxygen diffusion at anode, hampering the system with anolyte exhaustion. Also, the fermentative and methanogenic reactions that predominates in the system, limits the microbial metabolism, affecting the overall substrate utilization in MFCs [31-35]. MFC performance is directly related with microbial Coulombic efficiency (CE), which is the ratio between the total number of Coulombs obtained from the MFC as current to the total number of Coulombs added by the substrate.

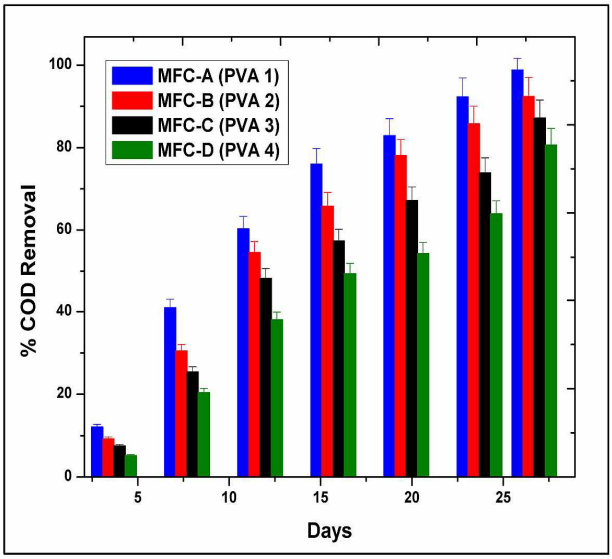

Fig.14. COD removal from MFCs

Lower CE (~1) was observed with MFC-A and B, which was due to the increased oxygen diffusion from cathode to anode, accounting for the substrate loss due to aerobic respiration and degradation in MFC-A and B. In contrast, with lower oxygen diffusion through PVA3 and PVA 4, improved current generation and better coulombic efficiency (~2.1) was achieved in MFC-C and MFC-D. Thus, an inverse relation between coulombic efficiency and COD removal was observed, indicating the efficiency of highly cross-linked membranes (PVA3 and PVA 4) over other membranes (PVA1 and PVA 2). This eventually corresponded with the microbial substrate adequacy, indicating the implication of cross-linked PVA membranes as an effective ion exchange barrier in MFCs with higher current and better coulombic efficiency. The lower manufacturing costs (~0.3 \$/100 cm^2) of cross-linked PVA membranes and their ability to generate high power output with increasing crosslink density enabled these membranes as promising membrane separators in MFC application for bioelectricity production.

MATERIALS AND METHODS

General Conditions

Poly vinyl alcohol (M_w = 115000 and DP= 1700-1800 and 98%- 99% degree of hydrolysis), Glutaraldehyde (25% solution) (Mol. Wt = 100.1g/mol), Sulphuric Acid (H_2SO_4), Acetic Acid (CH_3COOH), and Methanol (CH_3OH) were bought from Merck Millipore India. All chemicals were used as received. De-ionized (DI) water was used for all experiments. All microbial experiments and inoculations were performed under strict sterile conditions.

Preparation of acid catalyzed cross-linked poly vinyl alcohol membrane

The membrane of poly vinyl alcohol (PVA) was prepared by solution casting technique. For this, 3% (w/v) PVA solution was dissolved in distilled water at 90°C under a constant stirring condition for 6 hours. Varying concentrations of glutaraldehyde (GA) (0.1, 0.2, 0.4 and 0.6mL of 25% solution), as cross-linker was added in the PVA solution containing 0.05-0.3 mL of 10% solution of H_2SO_4 (as catalyst) , 0.15- 0.9 mL of 10% solution of acetic acid (pH controller), 0.1-0.6 mL of 50% solution of methanol (as a quencher) (Table 1). These were added in a 2:1:3:2 volumetric ratios prior to their addition to the PVA solution for the cross-linking of PVA and the solution was finally casted and dried at room temperature [36]. The cross-linked four membranes were designated as PVA 1, PVA 2, PVA 3 and PVA 4, which were further subjected for FT-IR, XRD, TGA, FESEM and tensile testing for analysis. Structure-composition and mechanical analysis were conducted to observe the effects of cross-linking on the membrane. Thermal tests were performed on a Thermogravimetric (TGA) Analyzer (ELTRA THERMOSET), (TA instruments, N_2 flow at 60 ml min^{-1}, heating rate of 10°C min^{-1}). The mechanical properties of the prepared membranes were determined using Universal Tensile Testing Machine (Nexygen *plus*, Lloyd instruments Ltd.), following the procedure of ASTM D 882- 02.

Table 1: Cross-linking composition of the PVA membranes.

Samples	Gluteraldehyde (ml)	Sulphuric Acid (ml)	Acetic Acid (ml)	Methanol (ml)
PVA 1	**0.1**	**0.05**	**0.15**	**0.1**
PVA2	**0.2**	**0.1**	**0.3**	**0.2**
PVA 3	**0.4**	**0.2**	**0.6**	**0.4**
PVA 4	**0.6**	**0.3**	**0.9**	**0.6**

Solvent Extraction

The degree of cross-linking in membranes was characterized by solvent extraction method [37]. Small pieces of the membranes were wrapped in filter paper and kept in distilled water at room temperature. The solvent was replaced in every 15 h until no further solubility was observed in the polymer. The remaining parts of the samples were dried and weighed. The gel fraction W (gel) of the membranes was calculated from Eq. (1):

$$W\ (gel) = W_1 / W_0 \times 100 \qquad (1)$$

Where, W_0 is the original weight of the dried membrane, and W_1 is the mass weight of the dried membrane after complete solvent extraction.

Water uptake and swelling study

Small pieces of membranes were kept overnight in deionized water. The dry and wet weights of membranes were utilized for water uptake calculation using the following equation:

$$\text{Water uptake } (\%) = (W_{wet} - W_{dry})\ (100)/W_{dry} \qquad (2)$$

Where, W_{wet} represents the weight of wet membranes obtained after soaking in DI water for 24 hrs, and W_{dry}, the weight of the respective dry membranes.

Similarly, swelling ratios of the prepared membranes were calculated from the following equation:

$$\text{Swelling Ratio (\%)} = (T_{wet} - T_{dry})\,(100)/T_{dry} \quad (3)$$

Where, T_{wet} represents the thicknesses of the wet membranes obtained after soaking in DI water for 24 hours, and T_{dry} is the thickness of the respective dry membranes.

Ion exchange capacity (IEC)

The ion exchange capacities (IECs) of the membranes were determined using conventional titration technique.

Protocol 1 [38, 39] : Square pieces of each membrane were soaked in a large volume of 1 M H_2SO_4 solution for 24 h. The samples were then repeatedly washed with distilled water in order to remove excess H_2SO_4. The samples were then placed in 50 mL of 1 M NaCl solution, heated to 40°C, and equilibrated for at least 24 h in order to replace the protons with sodium ions. The remaining solution was titrated with 0.01 N NaOH solution, using phenolphthalein as indicator. The IEC value (in meq g^{-1}) was calculated using the following equation (4):

$$IEC = V_{NaOH} \times S_{NaOH} / W_{dry} \quad (4)$$

where, V_{NaOH} is the volume of NaOH used in the titration, and W_{dry} is the dry weight of the membrane in g. S_{NaOH} is the strength of NaOH used in the experiment for determination of IEC.

Protocol 2 [40, 41, 42]: It is almost similar to protocol 1 except for sulphuric acid treatment. In this process, the samples were first treated with 1 M NaCl solution for 24 hr, followed by all necessary steps as in protocol 1.

Proton conductivity

The fully hydrated membranes were kept immersed in a 1 M H_2SO_4 solution for 24 h. Proton conductivity was measured at 25°C by the impedance spectroscopic technique in transverse direction of membranes, employing a potentiostat (Gamry Potentiostat-600) over a frequency range of 1 Hz to 10^5 Hz and at a potential of 10 mV (S2 Supporting information). The conductivities of the samples (r) were calculated from the respective impedance data, using the following equation:

$$\sigma = T/ R. A \quad (5)$$

where, T is the thickness of the sample, A is the cross-sectional area of the sample, R is the resistance derived from the low intersect of the high frequency semi-circle on a complex impedance plane with the real (Z) axis.

Preparation of membrane electrode assembly (MEA)

Carbon cloths (Zoltek pvt.Ltd, USA) of fixed dimension (6 cm^2) were kept overnight in de-ionized water to neutralize any unwanted interfacial ionic particles. Later, these were vacuum dried and used as electrodes (anode and cathode). In addition, a 10:90 wt% platinum:carbon (Pt/C) catalyst mixture mixed with 3% PVA solution was prepared. The obtained ink was paint coated on the carbon cloth at the cathode side, loading approximately a total of 3 $mgcm^{-2}$ of supported metal catalyst on the air facing side of cathode.

Cathodic reaction: $O_2 + 4e^- + 4H^+ \xrightarrow{Pt/C} 2H_2O$

Further, four sets of anode and cathodes with sandwiched membranes (PVA1, PVA2, PVA3 and PVA4) were assembled and hot pressed at 60°C for 5 minutes at 5 MPa pressure, resulting in four membrane electrode assemblies (MEAs). This optimum combination of time and temperature allows perfect membrane assembling, as above it, the membrane loses its texture due to high temperature rise.

MFC Configuration and Fabrication

In total, four identical single chambered MFC units namely, MFC- A-D of 150mL liquid volume (anode chamber) were constructed. MEAs containing PVA1, PVA2, PVA3 and PVA4 membranes were fitted in MFC-A, B, C and D respectively, where cathode side (doped with catalysts) facing outward were left open for direct air-exposure (Figure 15). Electrical connections with copper wires of ~1 ohm were made and requisite fabrications e.g. inlet/outlet sealing, electrode fixing etc were done properly to avoid leakage.

Oxygen Diffusivity Measurement

The mass transfer coefficient k (cm s^{-1}), as characterized by oxygen permeability was calculated from cathode to anode chamber over time, using the mass balance equation

$$k ¼ = - V /At \ln [C_s – C/ C_s] \quad (6)$$

Where, V is the anode chamber volume, A is membrane cross-sectional area, C is the anode oxygen concentration, and C_s is cathode oxygen concentration (assumed to be the saturation concentration of oxygen in water, or 7.8 mg L^{-1}). Oxygen concentrations were measured using a dissolved oxygen probe (Horiba Pvt. Ltd, Kyoto Japan) in the anode chamber. Prior to measurement, the water was purged with purified N_2 gas for the removal of dissolved oxygen and thereafter, the concentration of dissolved oxygen was periodically recorded to observe oxygen diffusivity.

Fig 15: Membrane electrode assembly (MEA) in single chambered MFCs

DNA isolation and PCR amplification

Genomic DNA isolation of pure culture isolates was done using standard phenol–chloroform method [43]. Isolated DNA was treated with RNase A, and its concentration was estimated by taking absorbance at 260 nm (UV spectrophotometer 2700, Thermo Scientific). 16S rRNA gene amplification were done by PCR (Applied biosystem, US) using universal primersY1Forward (40th) 5'-TGGCTC AGAACGAACGCGGCGGC-3' and Y2Reverse (337th) 5'-CCCACTGCTGCCTCC CGTAGGAGT-3'. Sequencing and BLAST tools were employed for identification of bacterial species and strains were allotted accession numbers.

Anolyte Preparation

Isolated microbial strains were firmicutes class lysinibacillus species (EMBL accession No. HE648059, HE648060, HF548664), which when tested for viability in gas pack jar were found facultative anaerobes. These mixed strains were suspended in 50 mM phosphate buffer (50 ml volume) and subsequently transferred to 100 ml synthetic wastewater (COD = 150 mg/L, pH = 7.0). The COD composition of the feed waste water was 1800±240 mg L^{-1} (total nitrogen: 114±27 mg L^{-1}, PO_4–P: 33±6 mg L^{-1}, $MgSO_4$:48 mg L^{-1}). Thus, a final volume of 150 mL (with microbe) anolyte was used as feed in MFCs.

MFC start-up, electrical parameters and measurements

Prior to operation, the assembled MFC units were stored in sterilized de-ionized water overnight, and later replaced by pumping anolyte using peristaltic pump. All MFCs were continuously monitored (24 h intervals) using a multimeter (Keithley Instruments, Cleveland, OH, USA), and a potentiometer (G600; Gamry Instrument Inc., Warminster, PA, USA) connected to a personal computer. Fuel cells were operated continuously for 28 days, where current (I) and potential (V) measurements were recorded after allowing the circuit to stabilize for 8–10 min. Power (W) was calculated using the relation P = IV, where I and V represents current and voltage, respectively. Power densities (mW/m^2) were calculated by dividing the obtained power by anode surface area. Substrate removal was analyzed by measuring chemical oxygen demand (COD) periodically at 420 nm (Anatech Labs India Pvt. Ltd., India). The measurements were done in triplicate. The Columbic efficiency (CE) of the fed-batch mode MFCs were calculated by applying the following formula:

$$CE = M \int_0^t I dt / FbV_{an} \Delta COD \qquad (7)$$

where 'M' represents the molecular weight of oxygen(M = 32), 'F' is Faraday's constant, 'b' denotes the number of electrons exchanged per mole of oxygen (b = 4), 'V_{an}' is the liquid volume in anode, and ΔCOD is the change in the chemical oxygen demand over time t.

Electrochemical impedance spectroscopy (EIS)

For internal resistance assessment, potentiostatic EIS was performed for all of the four MFCs at a frequency range of 10^3 kHz to 1 mHz at 10 mV. Nyquist graphs were plotted and the internal resistances of the MFCs (R_{in}) were determined [28].

Cyclic voltammetry (CV)

To analyze microbial electrochemical activity, CV was performed using a potentiostat with a scan rate of 2 mV/s (G600 Gamry Instrument Inc.,USA). The setup contained anode as the working, cathode as the counter, with an Ag/AgCl reference electrode, placed near the anode (for minimal iR drop). To ensure microbial activity, control experiments (without microbes) were conducted separately.

Scanning Electron Microscopy (SEM)

For confirming the microbial adhesion at electrode's surface, the bio-film containing electrode material was subjected for

SEM analysis. The bio-film developed on the electrode was fixed in 2.5% glutaraldehyde and 0.1 M phosphate buffer solution, and then dehydrated by using a continuously higher (from 30 to 100 %) concentration of ethanol [26]. The samples were dried, followed by sputter-coating with a thin layer of gold under vacuum to neutralize the charging effects. The morphology was observed under a scanning electron microscope (Carl Zeiss EVO® 18 electron microscope), using an acceleration voltage of 15 kV.

CONCLUSION

In summary, different cross-linked polyvinyl alcohol membranes with varied glutaraldehye concentration were compared as MEA in single chambered MFCs using mixed electrogenic firmicutes as biocatalysts. Increased cross-link density resulted in reductions in membrane properties (e.g., water uptake, swelling, IEC, proton conductivity) with lower oxygen diffusivity across membranes. 32% cross-linked membrane was found to be optimum as membrane barrier, where a maximum power and current density of 119.13 ± 6mWm^{-2} and 447.81 ± 18mAm^{-2} was observed with PVA3 fitted MFC. Further, cross-linking lowered MFC performance because of constricted ionic mobility with increased stiffness and reduced membrane pore size. Comparing the performance, approximately 83% higher power output was observed in PVA3 membrane over the least cross-linked membrane (PVA1). Being a cost effective approach, more such cross-linked PVA derivatives could potentially find a suitable role in future bioelectrochemical applications. MFC, being a future technology, demands more profound investigations in such diversified areas of membrane technology for relevant cost efficient practical alternatives.

ACKNOWLEDGEMENTS

The financial research aid provided from Council of Scientific and Industrial Research (CSIR), and Ministry of Environment and Forest, Govt. of India (MOEF) is duly acknowledged. Authors are acknowledging to Mr. Sujoy Debnath (Dept. of Polymer Science and Technology, CU ; XRD operator) , Mr. Samrat Kundu (CRNN, CU; FE-SEM operator), Mr. Ratul Bezbaruah (National Test House, Ministry of consumer affairs, Govt. of India; TGA operator) and also Mr. Nilkamal Pramanik, Arpita Nandy (senior research scholar of Advanced Polymer Laboratory, Technical and Experimental support).

Notes and References

Notes

[a] Authors have equal contribution.

Advanced Polymer Laboratory, Department of Polymer Science &Technology, 92 A. P. C. Road, University of Calcutta, Kolkata-700009.

**Corresponding author Fax & Tel: 91-33-2352-510;*

E-mail: ppk923@yahoo.com

The authors declare no competing financial interest.

References

1. D.L. Hoskins, X. Zhang, M.A. Hickner, B.E. Logan, Bioresour. Technol, 2014,172, 156–161.

2. Y. Hou, K. Li, H. Luo, G. Liu, R. Zhang, B. Qin, S. Chen, Environ. Sci. Eng, 2014, 8, 137–143.

3. S. Ayyaru, P. Letchoumanane, S. Dharmalingam and A. Stanislaus, J Power Sources 2012,217, 204–208.

4. S.Ayyaru and S. Dharmalingam, Bioresour Technol, 2011,102, 11167-11171.

5. S. Pandit, S. Ghosh, M. Ghangrekar and D. Das, Int J Hydrogen Energy, 2012, 37, 9383-9392.

6. M.Behera, P. Jana, T. More and M. Ghangrekar, Bioelectrochemistry, 2010, 79, 228-233.

7. Y. Fan, H.Hu and H. Liu, J Power Sources, 2007, 171, 348–354.

8. K.J.Chae, M.Choi, F.F.Ajayi, W.Park, I.S.Chang and I.S.Kim,Energy Fuels 2008, 22,169–176.

9. J.R.Kim, S.Cheng, S.E.Oh and B.E.Logan, Environ Sci Technol,2007, 41, 1004–1009.

10. H. Wang, S. J. Chen and J. Zhang, Colloid Polym Sci, 2009,287, 541–548.

11. M. Kaneko and H. Sato, Macromol Chem Phys, 2004, 205,173-178.

12. M. Kaneko and H. Sato, Macromol Chem Phys, 2005, 206, 456–463.

13. M. Kaneko, S. Kumagai, T. Nakamura and H. Sato, J Appl Polym Sci, 2004, 91, 2435–2442.

14. J. Ihata, J Appl Polym Sci: Part A: Polymer Chemistry, 1988, 26, 167–176.

15. B. Bolto, T Tran, M Hoang, Z Xie, Prog. Polym. Sci, 2009, 34, 969–981.

16. C. E. Tsai, C. W. Lin, B. J. Hwang, J Power Sources, 2010, 195, 2166–2173.

17. M. S. Kang, J. H. Kim, J. Won, S. H. Moon, Y. S. Kang, J. Membr. Sci., 2005,247, 127–135.

18. C. Chanthad, J. Wootthikanokkhan, J. Appl. Polym. Sci., 2006, 101, 1931–1936.

19. N. Seeponkai, J. Wootthikanokkhan, J. Appl. Polym. Sci., 2007, 105, 838–845.

20. J. M. Gohil, A. Bhattacharya, P. Ray, Journal of Polym. Res, 2006, 13, 161–169.

21. A. Anis, A.K. Banthia, S. Bandyopadhyay, 2008. ASM International; 10.1007/s11665-008-9200-1.

22. H.S. Mansur, CM. Sadahira, A. N. Souza, A.A.P. Mansur, Mater. Sci. Eng., C, 2008, 28, 539–548.

23. K. C. S. Figueiredo, T. L. M. Alves, C. P. Borges, J. Appl. Polym. Sci., 2009, 111, 3074–3080.

24. B. Smitha, S. Sridhar, A. A. Khan, J. Appl. Polym. Sci., 2005, 95, 1154–1163.

25. H. Strathmann, Membrane Sc. and Tech., 2004, series 9.

26. N. V. Bhat, M. M. Nate, M. B. Kurup, V. A. Bambole, S. Sabharwal, Nucl. Instr.and Meth. in Phys. Res, 2005, 237, 585–592.

27. K. Das, D. Ray, N. R. Bandyopadhyay,A. Gupta, S. Sengupta, S. Sahoo, A. Mohanty, M. Misra, Ind. Eng. Chem. Res., 2010, 49, 2176–2185.

28. C. C. Yang, Int. J. Hydrogen Energy, 2011, 36, 4419-4431.

29. H. Liu, S. Cheng and B. E. Logan. Environ Sci Technol, 2005, 39, 5488–5493.

30. Z. He and F. Mansfeld, Energy Environ Sci, 2009, 2, 215–219.

31. H.Liu, S.Cheng and B.E.Logan, Environ Sci Technol, 2005, 39, 5488–5493.

32. B. Min, J. Kim, S. Oh, J. Regan, J, B. E. Logan, Water Res., 2005, 39, 4961–4968.

33. Z.He, S.D.Minteer and L.T.Angenent, Environ Sci Technol, 2005, 39, 5262–5267.

34. J.Greenman, A.Ga´lvez, L.Giusti and I.Ieropoulos, Enzyme Microb Technol, 2009, 44,112–119.

35. C. I. Torres, A. M. Kato, B. E. Rittmann,Biotechnol Bioeng., 2008, 100, 872–881.

36. S. B. Kuila, S. K. Ray,P. Das, N. R. Singha, Chem. Process., 2011, 50, 391–403.

37. V. Kumar, P. Kumar, A. Nandy, P. P. Kundu. RSC Advances 2015,5, 30758-30767 DOI: 10.1039/C5RA03411F.

38. S. Das, P. Kumar, K. Dutta, P. P. Kundu. Appl. Energy, 2014, 113, 169-177.

39. K. Dutta, S. Das, P. Kumar, P. P. Kundu. Appl. Energy, 2014, 118, 183-191.

40. M. Zhu, B. He, W. Shi, Y. Feng, J. Ding, J. Li, F. Zeng. Fuel, 2010, 89, 2299–2304.

41. Chi-Yung Tseng, Yun-Sheng Ye, Kuei-Yu Kao, J. Joseph, Wei-Chung Shen, J. Rick, Bing-Joe Hwang, Int. J. Hydrogen Energy, 2011, 36, 11936-11945.

42. J. Qiao, T. Hamaya, T. Okada, Polymer , 2005, 46, 10809–10816.

43. A. Ghosh, B. Maity, K. Chakrabati and D. Chattopadhyay, Microb Ecol, 2007, 54, 452-459.

Graphical Abstract

Acid catalysed cross-linking of poly vinyl alcohol (PVA) by glutaraldehyde: Effect of crosslink density on the characteristics of PVA membrane used in single chambered microbial fuel cell

Ruchira rudra[a], Vikash Kumar[a], Patit Paban Kundu[*]

Advanced Polymer Laboratory, Department of Polymer Science &Technology, 92 A. P. C. Road, University of Calcutta, Kolkata-700009.

*Corresponding author Fax & Tel: 91-33-2352-510;

E-mail: ppk923@yahoo.com